Molecular Crystals and Liquid Crystals Science and Technology. Section A. Molecular Crystals and Liquid Crystals

Publication details, including instructions for authors and subscription information:
http://www.tandfonline.com/loi/gmcl19

Conduction ESR and Theoretical Studies of Graphite Intercalation by Nitric Acid

Albert Ziatdinov [a] & Peter Skrylnik [a]

[a] Institute of Chemistry, Far Eastern Branch of the Russian Academy of Sciences, 159, Prosp. 100-letija, 690022, Vladivostok, Russia

Version of record first published: 24 Sep 2006

To cite this article: Albert Ziatdinov & Peter Skrylnik (2000): Conduction ESR and Theoretical Studies of Graphite Intercalation by Nitric Acid, Molecular Crystals and Liquid Crystals Science and Technology. Section A. Molecular Crystals and Liquid Crystals, 340:1, 185-190

To link to this article: http://dx.doi.org/10.1080/10587250008025464

Mol. Cryst. and Liq. Cryst., 2000, Vol. 340, pp. 185-190
Reprints available directly from the publisher
Photocopying permitted by license only

Conduction ESR and Theoretical Studies of Graphite Intercalation by Nitric Acid

ALBERT ZIATDINOV and PETER SKRYLNIK

Institute of Chemistry, Far Eastern Branch of the Russian Academy of Sciences. 159, Prosp. 100-letija, 690022 Vladivostok, Russia

Results of an *in situ* conduction ESR (CESR) study of HNO_3 molecule intercalation into highly oriented pyrolytic graphite (HOPG) plate with width being comparable with the graphite skin-depth governed by c-axis conductivity are presented. The stepwise changes of the intensity of CESR signal from intercalated parts of the HOPG plate is clearly detected during the intercalation. Using the chemical potential vs. intercalation time offered by the authors for the experimental conditions, this dependence was calculated theoretically.

Keywords: graphite; intercalation; conduction ESR; HNO_3

INTRODUCTION

In spite of numerous publications devoted to studies of various aspects of graphite intercalation compounds (GICs) structure and properties[1,2], hitherto many aspects of mechanism of "guest" molecules intercalation into graphite have not received sufficient attention. CESR technique is one of the most powerful methods of studying graphite intercalation process, because shapes and intensities of the CESR signal both from non- and intercalated regions of graphite plate vary strongly during the intercalation. However, because of difficulty of similar experiments only a few CESR studies of graphite intercalation process have been undertaken[3-8]. But even in these cases, in consequence of presence of skin effect the interpretation of changing the graphite CESR signal during the intercalation process comes across on greater difficulties. This paper is devoted to the results 1) of an *in situ* CESR study of intercalation of HNO_3 molecules into HOPG plate with width being comparable with the graphite skin-depth δ_c governed by c-axis conductivity σ_c and 2) of the theoretical analysis of reasons for a stepwise evolution of the CESR signal intensity from intercalated part of graphite.

EXPERIMENTAL

CESR measurements were carried out at room temperature using an X-band spectrometer. The constant magnetic field ($\mathbf{H}_0$) modulation frequency and amplitude were 2.5 kHz and 0.1 mT, respectively. The experiments were carried out on HOPG plates with height (h)×width (l)×thickness (d) =0.4×0.04×0.02 cm^3, where l×h is the size of basal plane. The HOPG samples were held in a quartz tube connected via a valve to the reservoir with the intercalate (liquid HNO_3 with the density of ρ~1.565 g/cm^3). During the measurements $\mathbf{H}_0$ was applied along the graphite **c**-axis. According to data of the four-probe method, at 300 K the σ_c - conductivity of HOPG plate used is equal to 7.7 $\Omega^{-1}\cdot cm^{-1}$. In the X-band the value $\delta_c \sim l/2$ corresponds to this conductivity, i. e. the whole volume of the HOPG plate investigated was available for the CESR studies.

RESULTS

The CESR spectrum of HOPG plate consists of single asymmetric line determined by Dyson mechanism[9]. The spectrum is axial with respect to the **c** - axis and is characterized by $g_{\parallel}$=2.0474±0.0002 and $g_{\perp}$=2.0029±0.0002. The line asymmetry parameter, A/B, being determined as the maximum/minimum peak height ratio is 'normal' in the sense that the maximum peak height occurs at the lower magnetic fields and it is equal to 1.8.

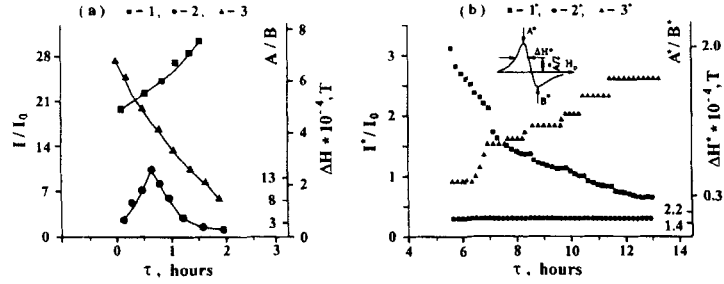

FIGURE 1 CESR lineshape parameters of non-intercalated (a) and intercalated (b) parts of the narrow (l~$2\delta_c$) HOPG plate vs. exposure time, τ, in HNO_3 atmosphere. 1(1*), 2(2*) and 3(3*) correspond to ΔH (ΔH*), A/B (A*/B*) and I/I_0 (I*/I_0), respectively. I [I*] = (A+B)×ΔH^2 [(A*+B*)×ΔH^{*2}]; I_0 is the intensity of the standard ESR signal.

Several minutes after the injection of HNO_3 gas into the part of reactor with the HOPG plate, the CESR signal of graphite begins to transform and decrease in intensity until it fully disappears. Simultaneously, in the spectrum a new signal with $g_{\parallel}$*=2.0019±0.0002, and $g_{\perp}$*=2.0030±0.0002 appears.

The linewidth (the intensity), ΔH ($I=(A+B)\times\Delta H^2$), of the graphite CESR signal increases (decreases) vs. exposure time, τ, monotonously (Fig. 1a). The A/B ratio of signal increases initially, but it is still 'normal' reaching a maximum value of A/B~13. Later, the A/B ratio is 'reversed' (maximum peak height occurs at higher magnetic fields), and its magnitude decreases down to ~2.

Early in the development of the reaction, a wide scattering of the intensity, $I^*=(A^*+B^*)\times\Delta H^{*2}$, and the linewidth, ΔH^*, values of the CESR signal with g_i^* ($i = \|, \perp$) is seen. As the time of reaction increases, this scattering decreases and both the I^* and ΔH^* vs. exposure time take a clearly defined stepwise form (Fig. 1b). The asymmetry ratio of signal, A^*/B^*, remains constant up to the end of the reaction.

DISCUSSION

At $\mathbf{H}_0$ oriented along the graphite **c**-axis microwave field penetrates into the HOPG plate mainly through its lateral sides, which are simultaneously parallel to both the **c**-axis and the magnetic component of microwave field[10], in our case through the sides ($h\times d$). Therefore, the evolution of the graphite CESR signal of the sample investigated (Fig. 1a) is mainly due to variations of the composition and properties of the HOPG plate at the surface areas from the lateral sides. To understand the nature of the observed CESR spectrum transformation of the (HOPG+HNO_3) system, it is necessary to note that the dependence of the shape and intensity of graphite CESR signal on exposure time is qualitatively identical to that of the CESR signal lineshape and intensity of the conductive substrate on the thickness of a spray-coated film of another metal[11]. It allows us to make the conclusion that the changes of A/B and I of the graphite CESR signal are determined by the formation of a macroscopic 'intercalation' layer from the lateral sides of the HOPG plate, and by the advance of the boundary which separates its intercalated and non-intercalated regions. We suppose that a reason for the significant broadening of the graphite CESR signal from the beginning of the reaction to the end of this phase of intercalation (Fig. 1a) is the collisions of graphite current carriers with the interface between the intercalated and the non-intercalated parts of the sample. It is necessary to note that in all previous ESR experiments on graphite intercalation[3-8] which were carried out on wide plates with $l \gg \delta_c$, the similar broadening of the graphite CESR signal were not observed. This fact is indirect evidence for offered by us interpretation of the graphite CESR signal broadening at intercalation of the narrow ($l\sim\delta_c$) graphite plate.

According to the X-ray diffraction data the first (last) 'plateau' in experimental dependence $I^*(\tau)$ (Fig. 1b) corresponds to the seventh (second) intercalation stage. Therefore, the number of steps in the $I^*(\tau)$ dependence is equal to the number of possible intercalation stages (small splitting of the second 'plateau' is neglected), and each step may be attributed to the definite stage. In our paper for the theoretical interpretation of the observed experimental dependence $I^*(\tau)$ analytical expressions for the stage fractions

calculation by Kirczenow[12] have been utilized. In that paper appropriate model of stage order and disorder as result of evolution of Daumas-Herold domains during intercalation process was presented. In the frameworks of that model calculation for the stage fractions f_i at given parameters (temperature, chemical potential, domain size etc.) may be fulfilled as follows[12]:

$$f_i = \exp(c_i), \qquad \left(\sum_i \exp(c_i) = 1\right) \tag{1a}$$

$$c_i = N_0 \ln N_0 - N \ln N - (N_0 - N)\ln(N_0 - N) - \frac{i\Psi}{kT} + \tag{1b}$$

$$+ \frac{1}{kT}\left(\mu\ N + \frac{\varepsilon\ z\ N^2}{2N_0} - \gamma\ N_0 - \frac{u_i N^2}{N_0}\right).$$

Expression (1b) was found from the minimization of the free energy Ψ with respect to the distributions f_i and in-plane density x of intercalate within domain ($x=N/N_0$). In (1) N_0 is the number of lattice-gas sites available to intercalate in any gallery within domain, N is the number of sites filled with intercalate, T is temperature, k is the Boltzmann constant, μ is the chemical potential, ε is the nearest neighbor in-plane interaction energy between intercalates and z is the in-plane coordination number, $u_i=\upsilon_0 i^{-\alpha}$ is the repulsive interaction between intercalate layers across i carbon layers, γ is the energy per lattice-gas site which is required to separate the host layers sufficiently to admit the intercalates. Having μ known and substituting other parameters to (1) we can obtain filling coefficient x and distribution f_i for the possible stages i. Then, resulting values let us estimate total amount of intercalate in GIC sample:

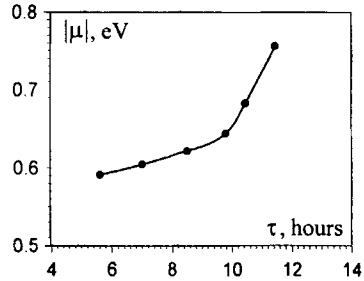

FIGURE 2 The chemical potential of the narrow HOPG plate, μ, vs. exposure time, τ, in HNO_3 atmosphere. Dots correspond to the threshold values μ_i and τ_i; solid line corresponds to the theoretical curve (3a).

$$M \propto \sum_i f_i\left(\frac{1}{i}\right)\frac{N}{N_0}. \tag{2}$$

In the experiment under consideration (the HOPG plate width $l \sim 2\delta_c$) CESR signal intensity I* increases with the amount of intercalate molecules in the sample increases, i.e. $I^* \propto M$. The problem of choice for $\mu(\tau)$ dependence, which is necessary for the $I^*(\tau)$ calculation using (2), is a non-trivial one. In the present paper, as well as Alstrom[13], we carried out the simulation of

intercalation process with introducing some dependence of chemical potential μ on time. It was supposed that during intercalation GIC system passes through a set of quasi-equilibrium states. The reason for such assumption was the following fact: in the considered experiment intercalation process is slow enough and the lifetime of definite stage greatly exceed the duration time of transitions between stages (Fig. 1b).

The reason for using in calculation of equilibrium states the analytical expressions (1) by Kirczenow[12] instead of those by Alstrom[13] in the frameworks of "devil's staircase" model, is the fact that expressions (1) take into account stage disorder phenomena. These phenomena are of importance in stage transitions[12], and confirmed by the numerical calculations of intercalation kinetics[14].

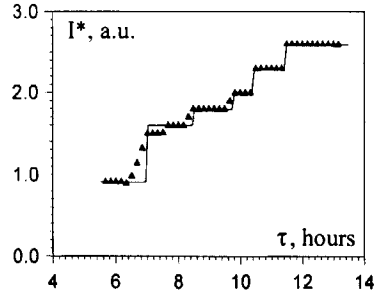

FIGURE 3 The experimental (dots) and the calculated (solid line) integral intensity, I*, of the CESR signal of intercalated parts of the narrow HOPG plate vs. exposure time, τ, in HNO_3 atmosphere.

Basing on the foregoing qualitative considerations the following procedure was used to obtain the dependence $\mu(\tau)$ corresponding to our experimental conditions. The threshold values of chemical potential, μ_i, which correspond to the stage transitions from stages with index $(i+1)$ to ones with index i, were calculated with expressions (1). Corresponding threshold time values τ_i have been determined from experiment. The results of such calculations are presented in Fig. 2.

The dependence $\mu_i(\tau_i)$ for our experiment (Fig. 2) qualitatively differs from one adopted by Alstrom[14] $\mu(\tau) = \mu_\infty\left(1-\exp(-\tau/\tau^*)\right)$, where μ_∞ is the μvalue at $\tau\to\infty$, τ^* is the 'relaxation' time. Probably, the reason for such deviation is the fact that aforementioned simple relaxation function is a good approximation for large exposure time only (see below). Therefore, we have used more general expression for $\mu(\tau)$ dependence:

$$\mu(\tau) = p'(\tau)\mu'(\tau) + p''(\tau)\mu''(\tau) \tag{3a}$$

with $$\mu'(\tau) = a\tau^{\beta} \quad \text{and} \tag{3b}$$

$$\mu''(\tau) = \mu_\infty(1-\exp(-\tau/\tau^*)), \tag{3c}$$

where a and β are some real numbers, $p'(\tau)$ и $p''(\tau)$ are the weight functions, meeting the condition: $p'(\tau)+p''(\tau) \equiv 1$.

In (3) the first term is dominating during the initial stages of intercalation, which are characterized by necessity of considerable pristine graphite deformation. The second term becomes dominating for the stages with low indices at the large time values. The formation of these stages requires large intercalate amount and, therefore, time. For these reasons functions $p'(\tau)$ and $p''(\tau)$ have been chosen as follows:

$$p'(\tau) = \exp(-\tau/\tau_0) \qquad \text{and}$$

$$p''(\tau) = 1 - \exp(-\tau/\tau_0),$$

where τ_0 is the characteristic time, at which transition from one mechanism to another takes place. In our case (Fig. 2) τ_0 is about 10 hours. The calculation results for $I^*(\tau)$ in the frameworks of the above-stated model (with the set of parameters[12]: N_0=300, $z\cdot\varepsilon$ =1eV, γ=1eV, υ_0=0.3eV, α=1) are shown in Fig. 3 and demonstrate a good agreement with experiment.

Acknowledgments

The authors are grateful to N.M. Mishchenko and V.V. Sereda for help in experiments and to L.B. Nepomnyashchii (Scientific Research Centre for Graphite, Moscow) for providing the HOPG. This work was supported by the Russian Foundation for Basic Research (grant № 97-03-33346).

References

[1] M.S. Dresselhaus and G. Dresselhaus, **30,** 139 (1981).
[2] P. Lagrange, A. Herold and C. Herold, *Mol. Cryst. Liq. Cryst.*, **310,** 33 (1998).
[3] R. Davidov, O. Milo, I. Palchan and H. Selig, *Synth. Met.*, **8,** 83 (1983).
[4] I. Palchan, D. Davidov, V. Zevin and G. Polatsek, *Phys. Rev. B,* **32,** 5554 (1985).
[5] I. Palchan, F. Mustachi, D. Davidov and M. Selig, *Synth. Met.*, **10,** 101 (1984/85).
[6] M. Nakajima, K. Kawamura and T. Tsuzuku, *J. Phys. Soc. Jpn.*, **57,** 1572 (1988).
[7] A.M. Ziatdinov, A.K. Tsvetnikov, N.M. Mishchenko and V.V. Sereda, *Mat. Sci. Forum,* **91/93** 563 (1992).
[8] A.M. Ziatdinov and N.M. Mishchenko, *J. Phys. Chem. Solids*, **58**, 1167 (1997).
[9] F.J. Dyson, *Phys. Rev.*, **98,** 349 (1955).
[10] A.M. Ziatdinov and N.M. Mishchenko, *Phys. Solid State (Russia),* **36,** 1283 (1994).
[11] V. Zevin and J.T. Suss, *Phys. Rev. B,* **34,** 7260 (1986).
[12] G. Kirczenow, *Phys. Rev. B.*, **31,** 5376 (1985).
[13] P. Alstrom, *Solid St. Comm.*, **56,** 1047 (1985).
[14] G. Kirczenow, *Phys. Rev. Lett.*, **55,** 2810 (1985).